JOC The Journal of Organic Chemistry

ARTICLE

pubs.acs.org/joc

Toward a Four-Toothed Molecular Bevel Gear with C_2-Symmetrical Rotors

Chen-Yi Kao,[†] Ya-Ting Hsu,[†] Hsiu-Feng Lu,[‡] Ito Chao,[*,‡] Shou-Ling Huang,[†] Ying-Chih Lin,[†] Wei-Ting Sun,[†] and Jye-Shane Yang[*,†]

[†]Department of Chemistry, National Taiwan University, Taipei, Taiwan, 10617

[‡]Institute of Chemistry, Academia Sinica, Taipei, Taiwan 11529

Supporting Information

ABSTRACT: The design, synthesis, conformational analysis, and variable-temperature NMR studies of pentiptycene-based molecular gears Pp_2X, where Pp is the unlabeled (in **1H**) or methoxy groups-labeled (in **1OM**) pentiptycene rotor and X is the phenylene stator containing ortho-bridged ethynylene axles, are reported. The approach of using shape-persistent rotors of four teeth but C_2 symmetry for constructing four-toothed molecular gears is unprecedented. In addition, the first example of enantioresolution of chiral pentiptycene scaffolds is demonstrated. Density functional theory (DFT) and AM1 calculations on these Pp_2X systems suggest two possible correlated torsional motions, geared rocking and four-toothed geared rotations, which compete with the uncorrelated gear slippage. The DFT-derived torsional barriers in **1H** for rocking, four-toothed rotation, and gear slippage are approximately 2.9, 5.5, and 4.7 kcal mol^{-1}, respectively. The low energy barriers for these torsional motions result from the low energy cost of bending the ethynylene axles. Comparison of the NMR spectra of **1OM** in a mixture of stereoisomers (**1OM**-mix) and in an enantiopure form (**1OM**-op) confirms a fast gear slippage in these Pp_2X systems. The effect of the methoxy labels on rotational potential energy surface and inter-rotor dynamics is also discussed.

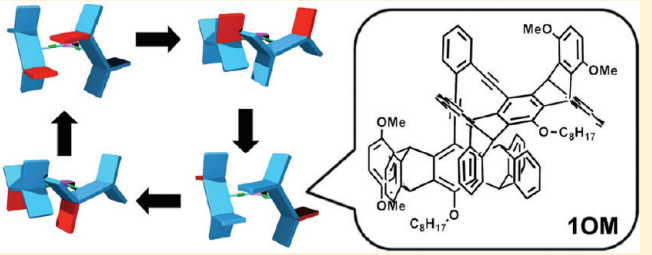

INTRODUCTION

The phenomenon of correlated rotary motions of two or more sterically congested groups in a molecule mimics the cogwheeling function of macroscopic gears.[1−6] The paradigms of molecular gearing systems are undoubtedly the three-toothed molecular bevel gears Tp_2X, where Tp represents the bridgehead-substituted triptycene rotors and X is the atom (e.g., O and S) or group (e.g., CH_2 and NH) stator.[1−3] These molecular gears possess a negligible energy barrier (1−2 kcal mol^{-1}) for disrotatory cogwheeling motions but high energy penalty (>20 kcal mol^{-1}) for uncorrelated rotations (i.e., gear slippage). It is desirable to construct molecular gears of larger number of gear teeth for more effective transmission of motions in artificial molecular machines.[5] However, previous attempts[6] have been impeded by the lack of suitable rotors of triptycene-like rigidity and shape persistency. In this context, we have explored the feasibility of pentiptycene (Pp),[7,8] a larger member of the triptycene family, being a four-toothed rotor, although its phenylene teeth are not of C_4 but C_2 symmetry.

In this paper, we report our first approach toward pentiptycene-based molecular gears Pp_2X through experimental and computational studies on the *o*-bis(ethynyl)benezene-bridged bipentiptycenes **1H** and **1OM**. Unlike the case of Tp_2X, AM1 calculations on both **1H** and **1OM** predict a higher barrier for four-toothed correlated rotation than for gear slippage and for geared rocking motions. Density functional theory (DFT) calculations also predict the same results on **1H**. Enantioresolution of the methoxy group-labeled pentiptycene building blocks was conducted to prepare optically pure isomer of **1OM** for NMR studies, the results of which confirm the computational prediction. The pros and cons of pentiptycene as a four-toothed rotor for constructing molecular gears are also discussed.

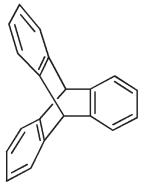

triptycene (Tp)

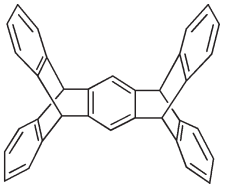

pentiptycene (Pp)

RESULTS AND DISCUSSION

Molecular Design. The great success of triptycene as a three-toothed rotor in molecular gears Tp_2X stems from its perfect structural symmetry and rigidity. Therefore, an ideal four-toothed

Received: May 4, 2011
Published: May 31, 2011

   dx.doi.org/10.1021/jo2009017 | *J. Org. Chem.* 2011, 76, 5782–5792

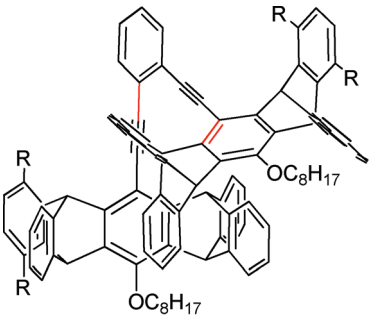

1H : R = H
1OM : R = OCH_3 (*S,S* enantiomer)

rotor for molecular gears should be C_4-symmetrical and shape-persistent. However, molecules that fulfill both criteria remain to be elusive. Previous approaches adopt C_4-symmetrical but shape-flexible rotors. The presence of intrarotor rotations in these systems not only complicates the inter-rotor rotational dynamics but also increases the chance of gear slippage, leading to unreliable geared rotations.[6] The alternative approach that uses non-C_4-symmetrical but shape-persistent rotors has not yet been reported. This prompts us to explore the potential utility of pentiptycene as a four-toothed rotor in Pp_2X. Like the case of triptycene, the scaffold of pentiptycene is shape-persistent and free from internal rotations of the phenylene teeth. However, unlike the presence of only V-shaped notches in triptycene, there exist both U-shaped and V-shaped notches in pentiptycene due to the C_2-symmetrical scaffold. This would result in two possible meshed forms (UU_4 and VV_4) during the four-toothed geared rotation (Figure 1, parts a and b). In addition, the twofold meshed form (UV_2), where the two teeth that form a V-notch in one rotor fit into the U-shaped notches of the other, cannot be ignored (Figure 1c). For the occurrence of gear slippage, there are two possible transition states, corresponding to the unmeshed UU and VV forms (Figure 1, parts d and e). The UU form is

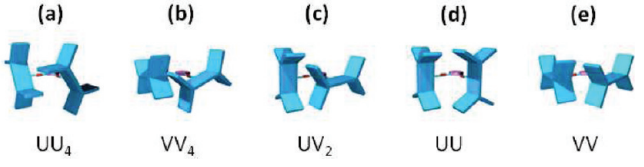

Figure 1. Schematic representation of the (a) UU_4, (b) VV_4, (c) UV_2, (d) UU, and (e) VV conformations of the two pentiptycene rotors in a Pp_2X system. The subscript numeric labels 2 and 4 in conformations a–c refer to the twofold and four-toothed intermeshed form, respectively. The conformations d and e are transition structures for gear slippage.

expected to have a shorter inter-rotor distance than the VV form. Despite the presence of several possible inter-rotor conformations, their relative energy can be readily evaluated by computations. In contrast, it is more difficult to track the dynamic interplay between intrarotor and inter-rotor rotations in systems of flexible rotors. This might highlight the advantage of shape-persistent rotors for constructing molecular gears.

The next concern is the stator X in Pp_2X. Pentiptycene is bulkier than triptycene and thus demands a larger spacing created by the stator X in Pp_2X versus that in Tp_2X. However, the distances between the axis of the rotor and the two faces of the U- and V-shaped notches are different in Pp, which results in different optimal inter-rotor distances for the UU_4 and VV_4 meshed forms (Figure 1, parts a and b). It appears that X should be somewhat flexible to accommodate both forms.

The target compounds **1H** and **1OM** were designed in part with the concern of synthetic feasibility. Among the known central-ring-functionalized pentiptycene building blocks,[9,10] the ethynylene- and octyloxy-substituted pentitpycene **2H** is particularly attractive in terms of synthesis, derivatization, shape, and solubility.[10] Compound **2H** could be readily synthesized from pentiptycene quinone **3H**, which is in turn prepared from benzoquinone and anthracene (Scheme 1).[11,12] The conversion of **2H** to **1H** could be accomplished through Sonogashira coupling reactions with 1,2-diiodobenzene. The linear ethynyl group in **2H** can function as an axle that allows free rotation of the Pp rotors and meanwhile as a spacer between the Pp rotors and the benzene stator. The ortho substitution brings the two Pp rotors in close proximity, as is the situation of *cis*-ethylene-bridged Tp_2X.[3] Very recently, a similar design in the axle–stator moiety was reported for molecular gears Tp_2X with X = 1,8-bis(ethynyl)naphthalene or 1,8-bis(ethynyl)anthracene.[13] The first combination of an ethynyl axle and a Tp rotor was employed to construct a prototype of molecular brakes.[14] The octyl groups in the pentiptycene rotors would ensure a good solubility for the target compounds. Moreover, to probe the inter-rotor rotational behavior in Pp_2X with NMR signals, it requires substituent labels on the teeth to break the symmetry and meanwhile to create stereoisomers. As such, the methoxy group-labeled species **1OM** is designed, because a facile synthesis of the precursor **3OM** starting from 1,4-dimethoxyanthracene and benzoquinone has been reported.[12]

Synthesis. The synthesis of target compounds is illustrated by the case of **1OM** (Scheme 2). Nucleophilic addition of lithium trimethylsilylacetylide to **3OM** followed by trapping of the phenoxide intermediate with trimethylsilyl (TMS) chloride and then by reductive aromatization of the central ring produced a racemic mixture of **4OM** as well as the TMS-capped precursors. The mixture was subjected to a basic condition for deprotection of the TMS group to afford a racemic mixture of **4OM**. Although

Scheme 1. Retrosynthesis of Molecular Gears 1H and 1OM

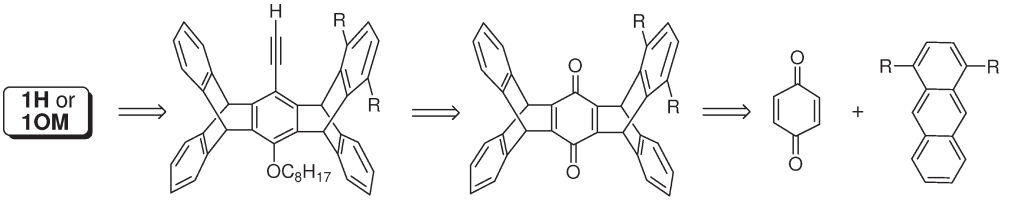

2H : R = H
2OM : R = OCH_3

3H : R = H
3OM : R = OCH_3

dx.doi.org/10.1021/jo2009017 |*J. Org. Chem.* 2011, 76, 5782–5792

Scheme 2. Syntheis of 1OM as a Mixture of Stereoisomers (1OM-mix)

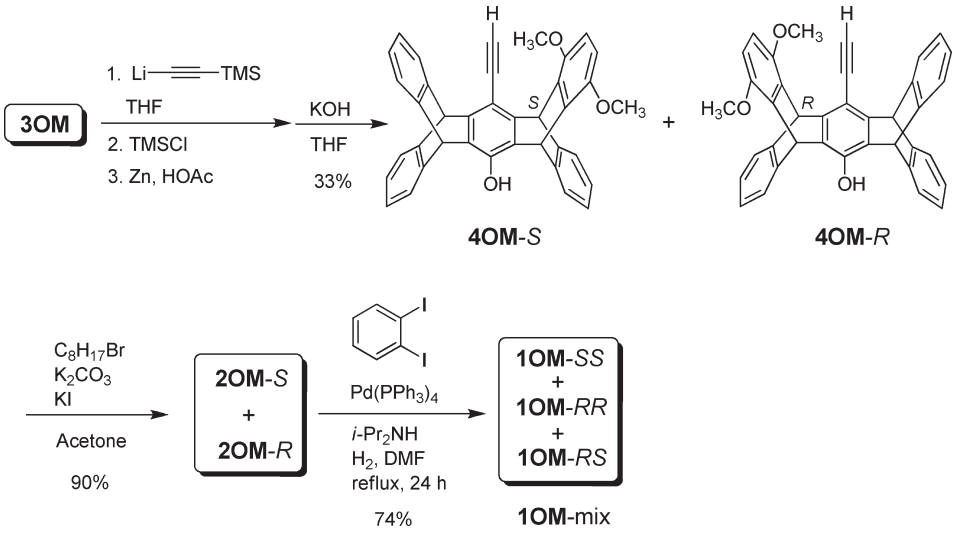

both the bridgehead carbons bonded to the dimethoxyphenylene tooth are stereogenic centers, the stereodescriptors *R*/*S* used herein for the compounds are based on the one close to the ethynyl group. Subsequent O-alkylation of **4OM** was conducted under a conventional S_N2 reaction condition. The resulting racemic mixture of **2OM** was reacted with 1,2-diiodobenzene to form the target compound **1OM** as a mixture of stereoisomers. This Sonogashira reaction requires the presence[15] of H_2 and the absence of copper catalyst to avoid the competition of the Glaser coupling reaction[16] between molecules of **2OM**. It should also be noted that the Sonogashira reaction condition is more rigorous (in reflux DMF vs THF at 60 °C) for the synthesis of **1OM** than for **1H**, presumably due to the bulkier **2OM** versus **2H**. We expect the presence of a statistical ratio of 1:1 for the meso (**1OM**-*RS*) and the racemic (**1OM**-*RR* and **1OM**-*SS*) isomers in the obtained **1OM**. This sample is called **1OM**-mix hereafter. Unfortunately, attempts to separate the diastereomers in **1OM**-mix by conventional silica gel column chromatography or by HPLC using columns made of chiral stationary phases were unsuccessful.

To obtain decisive conclusions from NMR studies (vide infra), data from optically pure **1OM** are required. In this context, we set out to resolve the racemates of **4OM** through formation of diastereomers with a chiral auxiliary. Very recently, it was shown that a camphanyl group attached to helical aromatic amide oligomers can result in a complete helix bias.[17] Indeed, the diastereomers derived from **4OM** and camphanic acid or camphor sulfonyl chloride can be separated by repeated HPLC on silica gel, which was the best, albeit not ideal, result among the chiral auxiliaries tested. We adopted camphanic acid for this work, since it is easier to cleave an ester C—O bond than a sulfonate S—O bond under a basic condition for removing the chiral auxiliary to recover **4OM**. As shown in Scheme 3, racemic **4OM** was converted to diastereomeric **5OM** by reacting with (−)-camphanic acid. The obtained diastereomeric mixture was separated by HPLC and then converted directly to enantiopure **2OM** through base-promoted ester hydrolysis and O-octylation. Figure 2a shows the mirror-imaged circular dichroism (CD) spectra of the enantiomers of **2OM** in THF. Although the

Scheme 3. Enantioresolution of 2OM through Diastereomer Formation with (−)-Camphanic Acid

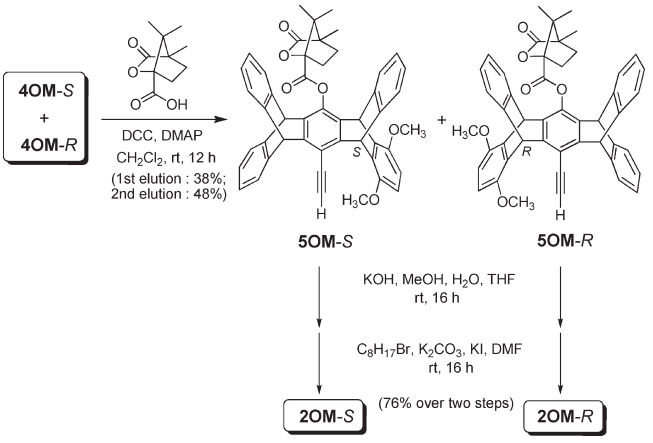

absolute configuration for each enantiomer of **2OM** is unknown at current stage, this does not affect our NMR analysis in this work. We adopted the enantiomer with a shorter elution time in HPLC and with the negative Cotton effects at the longest wavelength (303 nm) in CD for the construction of **1OM**. The product would be either **1OM**-*RR* or **1OM**-*SS* and is called **1OM**-op hereafter.

It is interesting to note that the CD signal for **1OM**-op (Figure 2b) is red-shifted and ca. 5 times stronger than that for enantiopure **2OM** under the same concentration of the **2OM** component (i.e., the concentration of **1OM**-op is half of that of **2OM**). This could be attributed to an increased π-conjugated length and molar absorptivity (Figure 2c) for the chromophores on going from **2OM** to **1OM**-op. The overall low CD intensity for both **1OM**-op and **2OM** reflects the "achiral" nature of the chromophores and a small perturbation in "molecular symmetry" by introducing the methoxy groups on one of the teeth.[18]

Rotational Potential Profiles. The rotational potentials of **1H** and all four stereoisomers of **1OM** have been investigated by computations. Since the length of the terminal alkyl chains is

dx.doi.org/10.1021/jo2009017 |*J. Org. Chem.* 2011, 76, 5782–5792

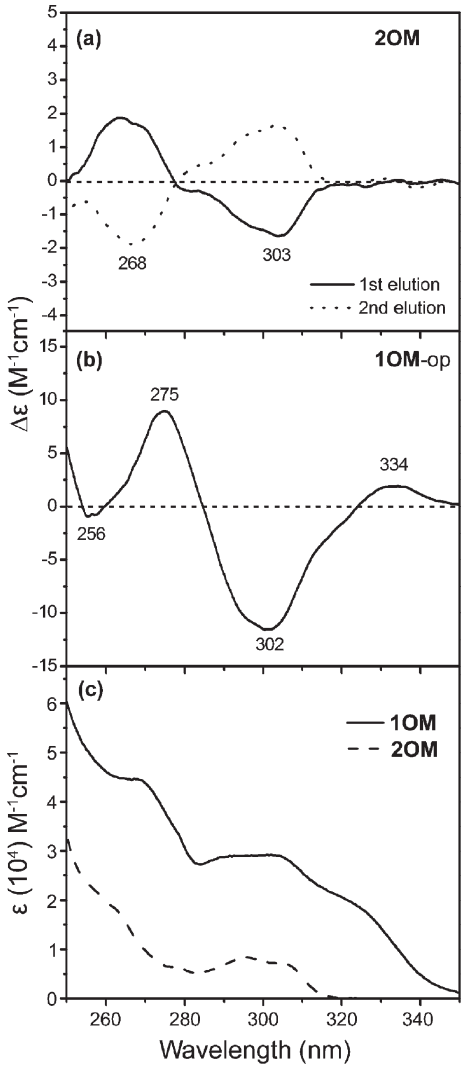

Figure 2. CD spectra of (a) enantiomers of **2OM** (5.32×10^{-5} M) and (b) **1OM**-op (2.66×10^{-5} M) and (c) UV spectra of **2OM** and **1OM**-op in THF recorded at room temperature.

irrelevant to this issue, the octyl groups were replaced by methyl groups to expedite the calculation. Figure 3a shows the geared rotational potential profile for **1H** derived from DFT calculations at the B3LYP/6-31G* level.[19] The optimized conformation of **1H** is a UU_4 geometry (conformer A, Figures 3b and 4). The dihedral angle (χ) defined by one of the axle−stator $C_{sp}-C_{sp2}$ bonds and the central ring of the other axle-connected pentiptycene group (see the red bonds in the structural formula of **1H**) in conformer A is −55.6°. The dihedral angle χ value can also be viewed roughly as the dihedral angle between the planes of the stator phenylene ring and the central ring of one of the pentiptycene rotors. For the purpose of discussion, this pentiptycene rotor is thereafter called the variable group (VG) and the other one is called the response group (RG). We calculated the rotational energies by constraining the dihedral angle χ to various increments of 10° from the optimized conformer A ($\chi = -55.6°$) in both clockwise and counterclockwise directions. It is noted that the ethynyl axles are relatively flexible and prone to slight bending whenever needed to relieve steric congestion. Therefore, when we rotate and constrain the VG at a certain dihedral angle, geometry optimization can lead to a structure resulting from rotation of the RG, bending of the ethynyl axle, or more likely, a combination of the two. In other words, multiple minima with close energies are possible for this molecule. The fact that various conformation combinations of the two terminal methoxy groups are possible also contributes to the multiple minima situation at a given χ (see Methods in Experimental Section). This is why the energy profile shown in Figure 3a is not completely symmetric.

The results shown in Figure 3a suggest two possible types of correlated torsional motions in **1H**: rocking and rotation. As schematically depicted in Figure 3b, the rocking motion interconverts the conformer A ($\chi = -55.6°$) and nearly its mirror form B ($\chi = 54.4°$) through the transition state I ($\chi = 4.4°$) that corresponds to the UV_2 form in Figure 1c. On going from conformer A to B, the VG rotates counterclockwise by 110° and the RG rotates clockwise by 64°, and it encounters an energy barrier of 2.9 kcal mol^{-1}. If the VG in conformer B continues to rotate counterclockwise, it would encounter a higher barrier of 5.5 kcal mol^{-1} by passing the transition state C ($\chi = 164.4°$) and then reach the ground state D ($\chi = -115.6°$). Further counterclockwise rotations of the VG would pass the transition state G and restore conformer B to finish a 360° rotation. In this case, the RG also undergoes a full 360° turn in an opposite (i.e., clockwise) direction. A nearly mirrored energy surface was found for the VG-clockwise geared rotation starting from conformer A. The detailed information about the changes in inter-rotor dihedral angles is shown in Figure S1 (see the Supporting Information). Overall, the A−E−F−H−A and B−C−D−G−B rotations accomplish a four-toothed geared rotation for **1H**. These geared rotations encounter the two possible meshed forms in Figure 1, parts a and b, where the UU_4 (isoenergetic conformers A, B, D, and F) and VV_4 (isoenergetic conformers C, E, G, and H) forms correspond to the ground states and transition states, respectively. A higher energy barrier by 2.6 kcal mol^{-1} for the rotation versus rocking (i.e., VV_4 vs UV_2) suggests that the latter would dominate (99%) the correlated inter-rotor rotations in **1H**. The energy data for conformers A−I are shown in Supporting Information Table S1.

The AM1 algorithm was also employed for the calculation of rotational potential of **1H** (Supporting Information Figure S2). Compared to the DFT results, the AM1 method provides essentially the same barrier (2.8 vs 2.9 kcal mol^{-1}) for the rocking motion but a slightly smaller barrier (5.0 vs 5.5 kcal mol^{-1}) for the fourth-toothed geared rotation. Regarding the similar results obtained for **1H** with both the DFT and AM1 methods, the corresponding calculations for **1OM** were carried out by the AM1 method only in order to expedite the calculations.

In the case of **1OM**, the geared rotational profile depends on the stereoisomers and phase isomers. Note that phase isomer refers to conformational isomers that possess high energy barriers for interconversion (i.e., extremely slow rate for gear slippage) in a molecular gear.[1,2] As schematically shown in Figure 5, there are totally four pairs of enantiomers, designated as *dl*1−*dl*4, when phase isomers are considered. The conformations in Figure 5 are represented by the UV_2 form, the transition state I in Figure 3b. This UV_2 conformation has the highest symmetry among the various meshed conformations when the methoxy labels are ignored (i.e., in **1H**).

Figure 6a shows the geared rotational profile of *dl*1 represented by **1OM**-SS_1. The corresponding energy data for conformers A−I and I′ are shown in Supporting Information Table S2.

dx.doi.org/10.1021/jo2009017 |*J. Org. Chem.* 2011, 76, 5782–5792

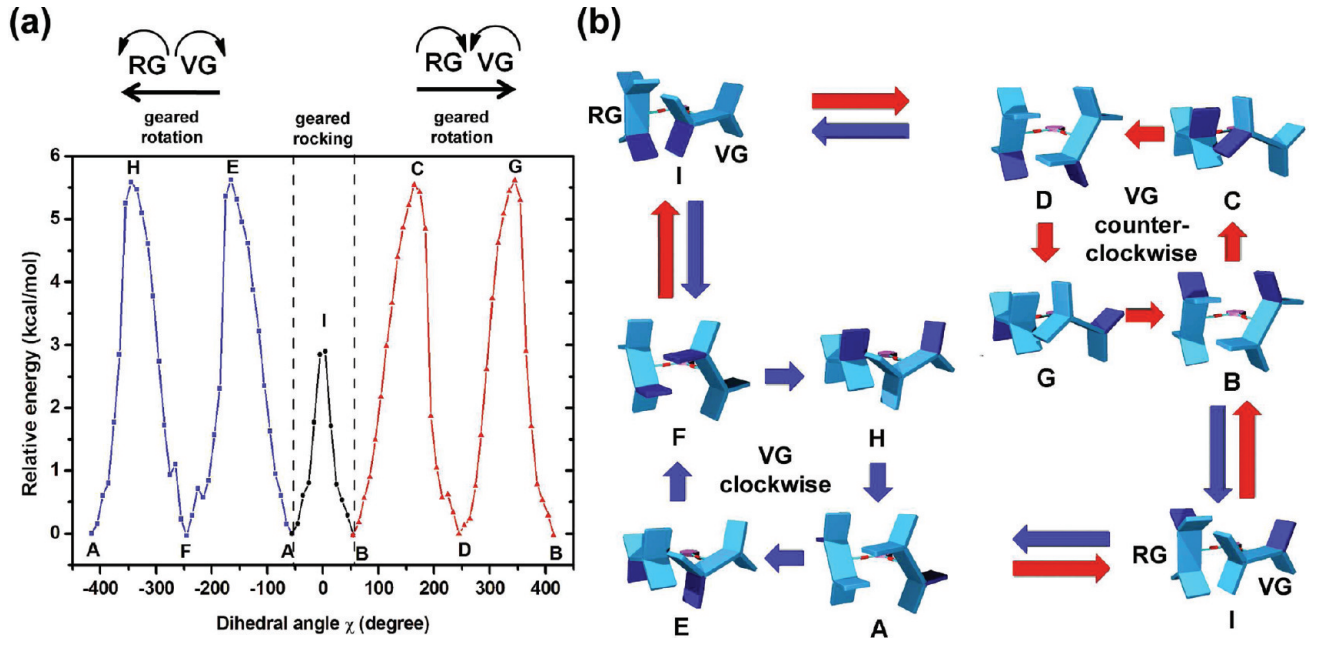

Figure 3. (a) DFT-derived rotational potential for geared rotational motions in **1H** and (b) schematic representation of the conformations at the ground and transition states. For clarity of conformational changes, one of the teeth in each rotor is labeled with blue color. The blue and red curves or arrows denote the clockwise and counterclockwise geared rotation potentials or conformations, respectively.

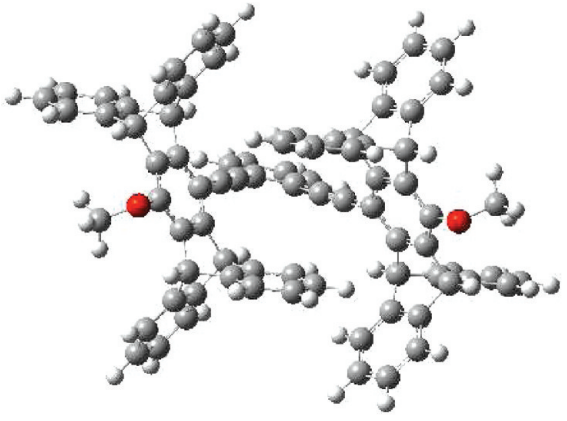

Figure 4. Fully optimized structure of conformer A of **1H** at the B3LYP/6-31G* level.

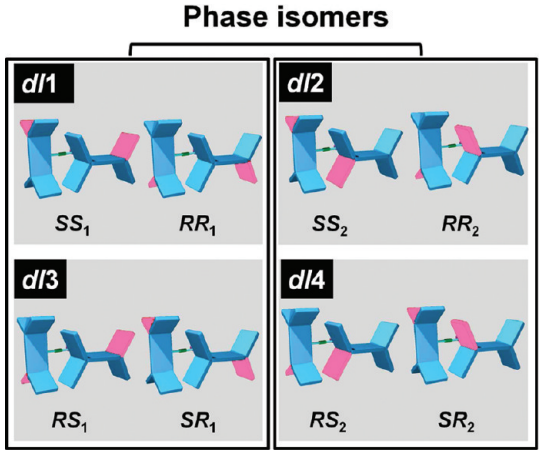

Figure 5. Schematic representation of the four groups (*dl*1−*dl*4) of stereoisomers of **1OM** in the UV_2 conformation. The methoxy-labeled phenylene teeth are in pink.

The decreased symmetry of rotational profile for **1OM** versus **1H** simply results from the presence of methoxy labels that increase steric hindrance in the meshed forms. The influence of the methoxy labels on rotational potentials can be seen in several respects. First, the energy of conformer C is the highest among the VV_4 forms due to a close proximity of the two methoxy group-labeled teeth. This results in a barrier as large as 12 kcal mol^{-1} for geared rotation from conformer B to D. Second, the VV_4 conformer G becomes a local minimum in the potential energy surface. Evidently, the steric interactions between the labeled and unlabeled teeth are larger in the transition states J and K than in the conformer G. In fact, in conformer G, two CH···O interactions can be found between the phenylene stator (X) and the methoxy groups of the labeled teeth (Supporting Information Figure S3a). Third, the steric effect is also present in the UU_4 ground states, as revealed by the destabilized conformer F relative to conformers A, B, and D. Finally, there are two different UV_2 transition states for the geared rocking motions. One is the transition state I between conformers A and B, and the other is transition state I′ between conformers D and F. The latter is less stable than the former by 2.5 kcal mol^{-1} again due to the close proximity of the two labeled teeth. We can conclude that the geared torsional motions are dominated by the rocking motions between conformers A and B, as is the case of **1H**. For the four-toothed geared rotations, the VG-clockwise rotation should be more favorable than the VG-counterclockwise rotation, since both the VV_4 transition states E and H in the former direction possess much lower energy than the VV_4 transition state C in the latter direction. These conclusions also apply to the *dl*2 group as represented by **1OM**-SS_2 (Supporting

dx.doi.org/10.1021/jo2009017 |*J. Org. Chem.* 2011, 76, 5782–5792

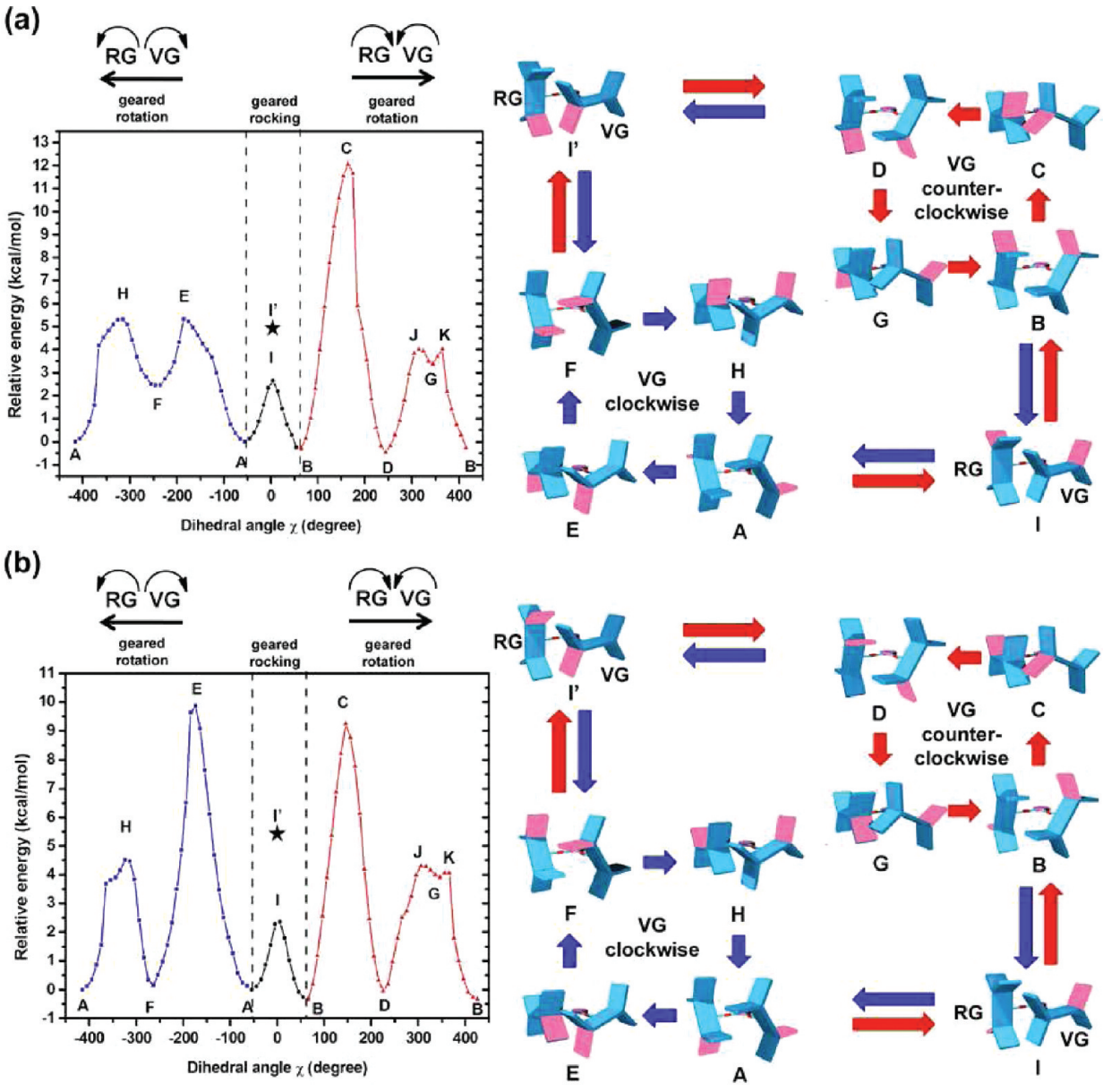

Figure 6. AM1-derived rotational potential and the corresponding schematic representation of the conformations at the ground and transition states for (a) **1OM**-*SS*$_1$ and (b) **1OM**-*RS*$_1$. The pink teeth represent the dimethoxy-substituted phenylene groups. The blue and red curves or arrows denote the clockwise and counterclockwise geared rotation potentials or conformations, respectively.

Information Figure S4), although the geared rocking is mainly between conformers D and F due to a lower UV$_2$ transition state I′ versus I (2.1 vs 6.2 kcal mol^{-1}).

The geared rotational potentials for the *dl*3 and *dl*4 are similar but somewhat different from those of *dl*1 and *dl*2. Figure 6b shows the case of *dl*3 by **1OM**-*RS*$_1$, and the results for *dl*4 by **1OM**-*SR*$_2$ are shown in Supporting Information Figure S5. According to Figure 6b, there are high barriers (ca. 9 kcal mol^{-1}) for both the VG-counterclockwise (transition state C) and VG-clockwise (transition state E) four-toothed geared rotation. The energy of transition states I and I′ for geared rocking are 2.4 and 5.6 kcal mol^{-1} relative to conformer A. Similarly, there is a local minimum for the VV$_4$ conformer G, which can be attributed to two CH···O interactions, one between the phenylene stator (X) and the methoxy group of the labeled teeth and the other between the labeled and unlabeled teeth (structure shown in Supporting Information Figure S3b). Thus, we can expect that the geared rocking between conformers A and B would be the most favorable geared motions, and a full 360° turn through four-toothed geared rotation would be negligible in these isomers.

On the basis of Figure 6, it can be concluded that in the VV$_4$ transition states, the steric effect of the methoxy-labeled tooth is significant when the tooth is located in the V-notch of the other rotor (e.g., conformer C in Figure 6a and conformers C and E in Figure 6b), but the steric perturbation is relatively small when the labeled tooth is outside of the V-notch, as evidenced by the similar energy of conformers C versus E and G versus H in Figure 6b. The fact that two of the four meshed forms in the four-toothed geared rotation are transition states (i.e., the VV$_4$ forms) renders this Pp$_2$X system a pseudo-four-toothed molecular bevel

dx.doi.org/10.1021/jo2009017 |*J. Org. Chem.* 2011, 76, 5782–5792

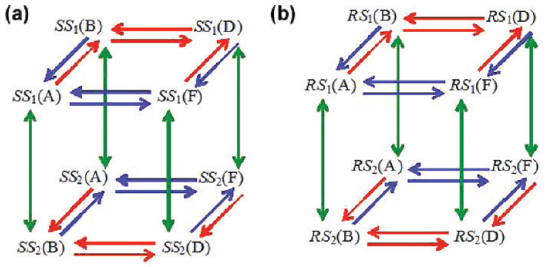

Figure 7. Schematic representation of relationship between phase isomers in (a) **1OM**-*SS* and (b) **1OM**-*RS*. The blue and red arrows denote the clockwise and counterclockwise geared rotation, respectively, within individual phase isomers, and the green double-headed arrows denote the UU gear slippage that interconverts phase isomers.

gear. This reveals the deficiency of the H-shaped pentiptycene scaffold[8] as a four-toothed rotor in constructing molecular gears.

In addition to the geared motions, the uncorrelated motions (i.e., gear slippage) for both **1H** and **1OM** are predicted to be also energetically feasible. For example, the conformer A of **1OM**-SS_1 can be converted to the conformer B of **1OM**-SS_2 by conrotatory motions of the rotors and through a UU transition state (Figure 1d). The barriers for a UU gear slippage were calculated to be 3−4 kcal mol^{-1} for **1OM** at the AM1 level (3.1, 3.4, 3.0, and 3.3 kcal mol^{-1} for SS_1(A) → SS_2(B), SS_2(A) → SS_1(B), RS_1(A) → RS_2(B), and RS_2(A) → RS_1(B), respectively) and 3.0 and 4.7 kcal mol^{-1} for **1H** by AM1 and DFT calculations, respectively. The slippage barrier through a VV transition state (Figure 1e), on the other hand, is 9.1 kcal mol^{-1} for **1H** by AM1 calculations. Therefore, slippage through a VV transition state is less viable. Schematic representations of the transition states are shown in Supporting Information Figure S6. The relationship between conformers of phase isomers is shown in Figure 7. The energy barrier for the UU gear slippage is higher than that for geared rocking but is lower than that for four-toothed geared rotations for **1H** and all the stereoisomers of **1OM**. Thus, the relative importance of the predicted internal rotation modes in both **1H** and **1OM** would be geared rocking > gear slippage > four-toothed geared rotation. To our knowledge, molecular systems of preferred geared rocking motions are unprecedented.[20] The occurrence of gear slippage at room temperature as well as at 183 K for **1OM** is indeed confirmed by NMR studies shown below.

Regarding the high rigidity of the pentiptycene rotors and the phenylene stator in these Pp_2X systems, the bendable ethynylene axles are responsible for the low barriers for both correlated and uncorrelated inter-rotor motions discussed above. The bending ability of an ethynyl group has been previously recognized,[21] although phenylene ethynylene conjugated oligomers and polymers are often called rigid-rod systems. The bond angles of the C_{sp2}(Ph)−C_{sp}−C_{sp} (α) and C_{sp}−C_{sp}−C_{sp2}(Pp) (β) in the calculated UU_4, VV_4, UV_2, and UU forms of **1H**, **1OM**-SS_1, and **1OM**-RS_1 at the AM1 level are shown in Supporting Information Table S3. Whereas the α and β values are close to 180° in the ground states (UU_4), a noticeable deviation from 180° is indeed present in the transition states of different modes of motion (VV_4, UV_2, and UU) with the largest deviation (165.3°) found in the conformer C of **1OM**-SS_1. The averaged α and β values are in the order UU_4 (176.8°) > UU (173.6°) ∼ UV_2 (173.3°) > VV_4 (170.8°). Evidently, the degree of bending in the ethynyl groups is strongly associated with the calculated energy, namely, the smaller the α or β value is, the higher is the energy of the conformer. Nevertheless, the energy cost for such bending is low.

NMR Spectra. Experimental verification of the computationally predicted inter-rotor motions in the current Pp_2X systems was carried out with NMR spectroscopy. Disregarding the inter-rotor rotation being geared or not, there is only one set of NMR signals for **1H** as long as the rotation is fast on the NMR time scale. Indeed, the presence of only one set of ^{1}H NMR signals even at a temperature as low as 183 K for **1H** in CD_2Cl_2 (Supporting Information Figure S7) is consistent with the predicted low energy barriers for geared rocking and four-toothed geared rotation as well as for uncorrelated rotations of the pentiptycene rotors.

In contrast, the NMR spectrum of **1OM** depends not only on the number of stereoisomers but also on the presence or absence of phase isomers in the sample. In the presence of phase isomers (i.e., gear slippage is slow on the NMR time scale), four sets of NMR signals are expected for **1OM**-mix, corresponding to the four pairs of enantiomers *dl*1−*dl*4 in Figure 5, and it becomes of only two sets (*dl*1 and *dl*2) for **1OM**-op. In the absence of phase isomers (i.e., gear slippage is fast and thus *dl*1 = *dl*2 and *dl*3 = *dl*4), two and one set(s) of NMR signals are expected for **1OM**-mix and **1OM**-op, respectively. This analysis assumes that each pair of enantiomers *dl*1−*dl*4 has distinct resonances. However, the possibility cannot be excluded that some of the stereoisomers might happen to be isochronous (i.e., a fortuitous coinciding of all resonances). This concern is raised from inspecting the conformations I and I′ in *dl*1−*dl*4, which can be divided into two groups. The first group consists of *dl*1 and *dl*3 that contain the labeled teeth pointing inward (conformer I′) or outward (conformer I) simultaneously (Figure 6, parts a and b). In contrast, the conformers I and I′ in the second group of *dl*2 and *dl*4 always possess one of the two labeled teeth pointing inward the other one outward (Supporting Information Figures S4 and S5). If *dl*1 and *dl*3 were isochronous and so were *dl*2 and *dl*4, then **1OM**-mix and **1OM**-op would both display two sets of NMR signals in the presence of phase isomers and one set of NMR signals in the absence of phase isomers. Therefore, comparison of the NMR spectra of **1OM**-mix and **1OM**-op can provide an unambiguous determination of the gearing effect in this Pp_2X system.

Figure 8a shows the ^{1}H NMR spectra for **1OM**-mix and **1OM**-op in DMF-d_7 at room temperature. There are two sets of signals of equal intensity for **1OM**-mix and one set of signals for **1OM**-op that coincides with the resonances of one of the two sets for **1OM**-mix. Evidently, the stereoisomers of **1OM** have distinct resonances and the current Pp_2X system does not possess phase isomers at room temperature. The latter is consistent with the low barriers calculated for gear slippage (vide supra). On the basis of a series of 2D NMR experiments, including COSY, HSQC, HMBC, NOESY, and ROESY, and the assumption that the methoxy-labeled teeth possess a larger ring current than the unlabeled teeth,[22] all the signals for **1OM**-op can be unambiguously assigned (Supporting Information Figures S8−S14). It is interesting to note that the chemical shifts for H_c and $H_{c'}$ in **1OM**-*SS*/**1OM**-*RR* are slightly upfield-shifted than those in **1OM**-*RS*.

Figure 8b shows the variable-temperature (VT) ^{1}H NMR in the pentiptycene region for **1OM**-op in DMF-d_7. More complete VT NMR spectra are shown in Supporting Information Figure S15. As is the case of **1H**, the number of signals for **1OM** is unchanged at all temperatures. The absence of peak splitting at low temperatures is again consistent with the calculated low barrier for gear slippage. It is interesting to point out that upon

dx.doi.org/10.1021/jo2009017 |J. Org. Chem. 2011, 76, 5782–5792

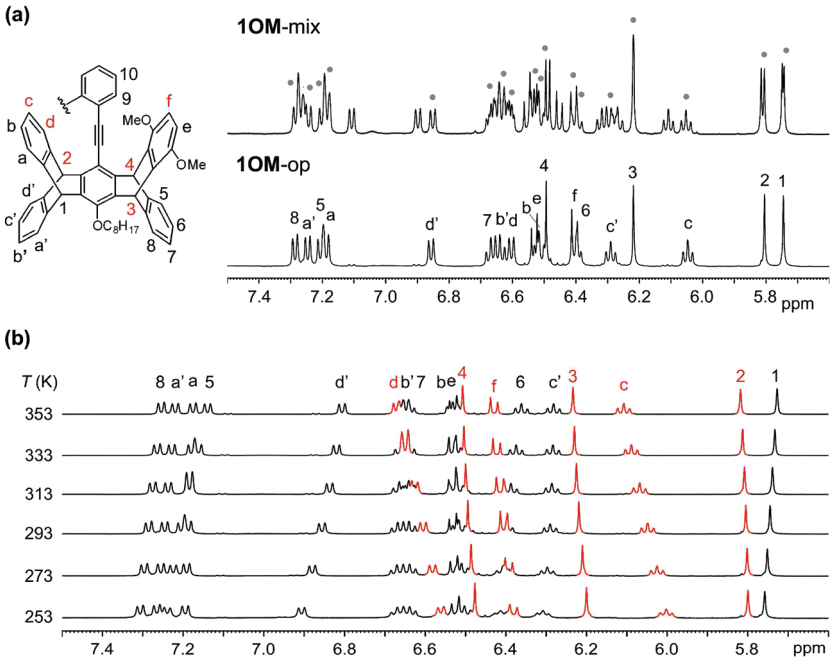

Figure 8. Pentiptycene region of the (a) ^{1}H NMR spectra (500 MHz) of **1OM**-mix and **1OM**-op in DMF-d_7 at 293 K and (b) VT ^{1}H NMR spectra (500 MHz) of **1OM**-op in DMF-d_7. Temperature (T, K) is given for every trace. The solid circles in the spectra of **1OM**-mix denote the signals from **1OM**-op.

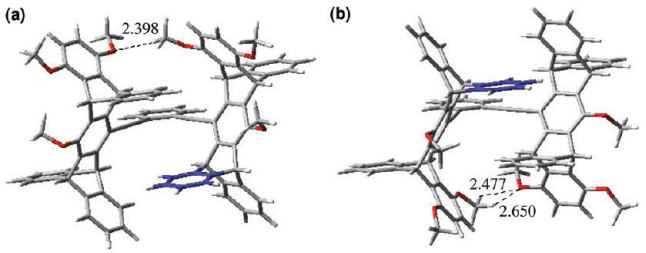

Figure 9. AM1-derived ground-state conformers (a) B and (b) D for **1OM**-SS_1. The ring bearing H_c and H_d is marked with blue color. Selected distances (in angstroms) are shown.

lowering the temperature most of the signals are either unmoved or downfield-shifted except for the nuclei H_2, H_3, H_4, H_c, H_d, and H_f (red peaks) that undergo an upfield shift. A shielding of the latter nuclei can be expected when they are located in the U-notch of the other rotor in the UU_4 conformation. This is indeed consistent with the AM1-derived rotational profile for **1OM**-SS_1 (Figure 6a), where conformers B and D are predicted to be more stable UU_4 forms. The nuclei H_2, H_c, and H_d in the VG rotor are located in the U-notch of RG in conformer B and vice versa in conformer D. Figure 9 shows the AM1-optimized conformers B and D (Figure 6a). They both show CH···O interactions between methoxy groups on different rotors. This probably explains why they are preferred conformers over conformer A. Since these lower-energy UU_4 conformers would be enriched at lower temperatures, the shielding effect of the U-notch phenylene teeth on nuclei H_2, H_c, and H_d would become more significant.

CONCLUSION

The inter-rotor rotation modes in the teeth-unlabeled **1H** and teeth-labeled **1OM** have been investigated in order to evaluate the potential utility of pentiptycene as a four-tooth rotor in constructing four-toothed molecular bevel gears (Pp_2X). Our approach differs from the previous ones in terms of the symmetry of rotors. Unlike the previous approach of using rotors of n teeth and n-fold symmetry for n-toothed molecular gears,[1−6] the current approach adopted twofold symmetrical pentiptycene rotors for four-toothed gears. This mismatch in teeth number and molecular symmetry results in a less favorable four-toothed geared rotation than the other inter-rotor motions such as geared rocking or gear slippage in both **1H** and **1OM**. Nevertheless, the rotational potential of a Pp_2X system appears to be adaptable through teeth substitutions to favor the four-toothed geared rotation in view of (a) the small difference of 1−2 kcal mol^{-1} among the rotational barriers in the different modes and (b) the significant perturbations of teeth labeling on the rotational barriers. Further studies on the replacement of stator/axle units and the influence of substituents in the inter-rotor rotation modes of this Pp_2X system are ongoing in our laboratory.

EXPERIMENTAL SECTION

Methods. The actual sample temperature for variable-temperature NMR measurements was calibrated by ^{1}H signals of ethylene glycol and methanol, and the temperature error was assured to be within ±1 K. Signal acquisition was begun after a sufficient temperature equilibration time (10−15 min). The calculations were performed with the Gaussian03 and Gaussian09 programs.[23] Using the fully optimized structure of conformer A, automated scans for rotational profiles with constrained optimizations were performed with opt = addredundant. The structure of conformer A of **1H** is shown in Figure 4. The dihedral angle (χ) used to scan the rotational profile was defined in text and their values are −55.6° and −56.29° at the B3LYP and AM1 levels, respectively. A sample input file for AM1 clockwise scan of **1H** with an angle increment of 10 is provided in the Supporting Information (Figure S16). Ideally, the number of automated steps (*nsteps*) in a scan can be set to cover the whole range of dihedral angles of interest. Nevertheless, certain constrained

dx.doi.org/10.1021/jo2009017 |J. Org. Chem. 2011, 76, 5782–5792

optimizations may fail or produce irrelevant structures, resulting in missing or irregular points in the rotational profile. When these situations occurred, a subsequent scan was initiated, starting with the successfully constrained optimized structure that is close to the missing/irregular point on the profile. It is noted that the methoxy groups of **1H** in Figure 4 are both pointing away from the gear center. Because energies of local minima with different combinations of methoxy conformations vary by only 0.13 and 0.03 kcal mol^{-1} for conformer A of **1H** at the AM1 and B3LYP/6-31G* levels, the structure shown in Figure 4 was used for all scans of **1H** and **1OM**. For **1OM**, additional methoxy groups are present on the labeled teeth. These groups are also oriented away from the gear center in the initial structure, so as to avoid bumping into the bridgehead proton in pentiptycene.

Materials. Compounds **2H**,[10] **3H**,[10] and **3OM**[12] were prepared according to the literature procedures. The synthetic procedures and characterization data for the other compounds are shown in the following.

Synthesis of 1H. To a mixture of **2H** (0.10 g, 0.18 mmol), $Pd(PPh_3)_4$ (0.02 g, 0.017 mmol), and 25 mL of dry THF was added 1,2-diiodobenzene (2 mL of 0.038 M benzene solution, 0.08 mmol) and 5 mL of diisopropylamine under N_2/H_2 (1:1). The mixture was refluxed for 16 h. The mixture was cooled and then extracted with CH_2Cl_2. The organic layer was dried over anhydrous $MgSO_4$, and the filtrate was concentrated under reduced pressure. Column chromatography with CH_2Cl_2/hexane (1:4) as eluent afforded the white solid of **1H** with a yield of 66%: mp, 294−296 °C; ^{1}H NMR (500 MHz, CD_2Cl_2) δ, 0.96 (t, J = 7.0 Hz, 6H), 1.39−1.55 (m, 16H), 1.68−1.71 (m, 4H), 2.02−2.05 (m, 4H), 4.02 (t, J = 6.8 Hz, 4H), 5.61 (s, 4H), 5.80 (s, 4H), 6.32 (t, J = 7.4 Hz, 8H), 6.62 (t, J = 7.4 Hz, 8H), 6.35 (d, J = 7.3 Hz, 8H), 7.14 (d, J = 7.3 Hz, 8H), 7.64−7.66 (m, 2H), 8.01−8.03 (m, 2H); ^{13}C NMR (125 MHz, CD_2Cl_2) δ, 14.5, 23.3, 27.0, 30.0, 30.2, 30.3, 31.1, 32.5, 48.7, 52.8, 76.8, 89.3, 93.9, 111.3, 123.6, 124.0, 125.2, 125.3, 127.1, 129,1, 133.2, 136.2, 145.1, 145.4, 146.9, 150.5; IR (KBr) 3066 (C═C−H), 2925 (C−H), 2204 (C≡C), 1575 (C═C) cm^{-1}; HRMS calcd for $C_{94}H_{78}O_2$, 1238.6002; found, 1238.6006.

Synthesis of 1OM-mix and 1OM-op. To a mixture of racemic or enantiopure **2OM** (0.22 g, 0.34 mmol), $Pd(PPh_3)_4$ (0.03 g, 0.026 mmol), and 10 mL of DMF was added 1,2-diiodobenzene (3.4 mL of 0.038 M benzene solution, 0.08 mmol) and 4 mL of diisopropylamine under N_2/H_2 = (1:1). The mixture was kept stirring at 60 °C for 16 h. The mixture was cooled and then extracted with CH_2Cl_2. The organic layer was dried over anhydrous $MgSO_4$, and the filtrate was concentrated under reduced pressure. Column chromatography with CH_2Cl_2/hexane (1:3) as eluent afforded the white solid of **1OM** with a yield of 74%. **1OM**-mix: mp, 189−250 °C; ^{1}H NMR (800 MHz, DMF-d_7) δ, 0.92−0.93 (m, 12H), 1.37−1.52 (m, 32H), 1.69−1.71 (m, 8H), 2.03−2.05 (m, 8H), 3.64 (s, 6H), 3.66 (s, 6H), 3.81 (s, 12H), 4.06−4.09 (m, 4H), 4.12−4.15 (m, 4H), 5.76 (s, 2H), 5.77 (s, 2H), 5.82 (s, 2H), 5.83 (s, 2H), 6.07 (t, J = 7.3 Hz, 2H), 6.13 (t, J = 7.3 Hz, 2H), 6.24 (s, 4H), 6.29 (t, J = 7.3 Hz, 2H), 6.31 (t, J = 7.3 Hz, 2H), 6.34 (t, J = 7.3 Hz, 2H), 6.41−6.43 (m, 4H), 6.47 (d, J = 8.7 Hz, 2H), 6.50 (s, 2H), 6.51 (s, 2H), 6.53−6.58 (m, 8H), 6.62−6.70 (m, 12H), 6.87 (d, J = 7.2 Hz, 2H), 6.92 (d, J = 7.2 Hz, 2H), 7.13 (d, J = 7.2 Hz, 2H), 7.21 (d, J = 7.0 Hz, 4H), 7.25 (d, J = 7.2 Hz, 2H), 7.26 (d, J = 7.3 Hz, 2H), 7.28−7.31 (m, 6H), 7.81−7.82 (m, 4H), 8.14−8.15 (m, 4H); ^{13}C NMR (200 MHz, DMF-d_7) δ, 14.8, 23.6, 27.2, 31.3, 32.9, 42.8, 46.9, 46.9, 48.8, 53.3, 56.9, 57.3, 57.3, 77.1, 89.7, 89.7, 94.6, 94.6, 110.2, 110.2, 110.7, 110.8, 111.8, 124.1, 124.1, 124.1, 124.2, 124.4, 124.5, 124.6, 124.8, 125.5, 125.5, 125.6, 125.7, 125.7, 125.8, 125.8, 125.8, 125.9, 126.8, 130.3, 134.1, 134.2, 135.5, 136.1, 137.1, 137.3, 137.4, 145.6, 145.7, 145.8, 145.9, 146.0, 146.0, 146.1, 146.2, 146.2, 146.2, 147.4, 147.4, 148.0, 149.9, 149.9, 150.2, 150.2, 151.1; IR (KBr) 3066 (C═C−H), 2926 (C−H), 2204 (C≡C), 1579 (C═C) cm^{-1}; HRMS calcd for $C_{98}H_{86}O_6$, 1358.6424; found, 1358.6399. **1OM**-op: mp, 189−191 °C; $[\alpha]_D^{25}$ +5.1° (c = 1, CH_2Cl_2); ^{1}H NMR (500 MHz, DMF-d_7) δ, 0.90 (t, J = 6.9 Hz, 6H), 1.37−1.34 (m, 8H), 1.44−1.42 (m, 4H), 1.52−1.46 (m, 4H), 1.71−1.65 (m, 4H), 2.07−1,98 (m, 4H), 3.62 (s, 6H), 3.79 (s, 6H), 4.14−4.03 (m, 4H), 5.74 (s, 2H), 5.80 (s, 2H), 6.05 (t, J = 7.2 Hz, 2H), 6.22 (s, 2H), 6.29 (t, J = 7.2 Hz, 2H), 6.41−6.38 (m, 4H), 6.49 (s, 2H), 6.51 (t, J = 8.4 Hz, 2H), 6.53 (d, J = 8.9 Hz, 2H), 6.60 (d, J = 7.2 Hz, 2H), 6.68−6.62 (m, 4H), 6.86 (d, J = 7.2 Hz, 2H), 7.19 (d, J = 8.4 Hz, 2H), 7.20 (d, J = 8.4 Hz, 2H), 7.25 (d, J = 7.2 Hz, 2H), 7.28 (d, J = 7.3 Hz, 2H), 7.79 (dd, J = 5.7 and 3.3 Hz, 2H), 8.12 (dd, J = 5.7 and 3.3 Hz, 2H); ^{13}C NMR (125 MHz, DMF-d_7) δ, 14.3, 23.2, 26.7, 30.9, 32.4, 42.3, 46.4, 48.3, 52.8, 56.4, 56.8, 76.7, 89.2, 94.1, 109.7, 110.2, 111.3, 123.6, 123.7, 123.9, 124.0, 124.1, 124.4, 125.1, 125.2, 125.2, 125.3, 125.4, 125.4, 126.4, 129.8, 133.7, 135.0, 135.6, 136.6, 136.9, 145.2, 145.3, 145.4, 145.5, 145.7, 145.8, 146.9, 147.5, 149.4, 149.8, 150.6, 162.5, 162.7, 162.9; IR (KBr) 3066 (C═C−H), 2926 (C−H), 2204 (C≡C), 1579 (C═C) cm^{-1}; HRMS calcd for $C_{98}H_{86}O_6$, 1358.6424; found, 1358.6429.

Synthesis of Racemic 2OM. A mixture of racemic **4OM** (1.0 g, 1.9 mmol), 1-bromooctane (0.27 mL, 2.0 mmol), K_2CO_3 (0.49 g, 3.6 mmol), and KI (0.31 g, 1.9 mmol) in 25 mL of dry acetone was refluxed for 3 days. The solution was cooled, the solvent was removed under reduced pressure, and the residue was dissolved in CH_2Cl_2 and washed with brine. The organic layer was dried over anhydrous $MgSO_4$, and the filtrate was concentrated under reduced pressure. Column chromatography with CH_2Cl_2/hexane (2:1) as eluent afforded the white solid. The crude product was recrystallized from CH_2Cl_2/MeOH to afford the white solid of **2OM** with a yield of 90%: mp, 242−244 °C; ^{1}H NMR (400 MHz, $CDCl_3$) δ, 0.95 (t, J = 6.8 Hz, 3H), 1.37−1.52 (m, 8H), 1.64−1.68 (m, 2H), 1.99−2.03 (m, 2H), 3.58 (s, 1H), 3.76 (s, 3H), 3.78 (s, 3H), 3.89−3.91 (m, 1H), 3.99−4.02 (m, 1H), 5.66 (s, 1H), 5.82 (s, 1H), 6.12 (s, 1H), 6.28 (s, 1H), 6.43−6.49 (m, 2H), 6.89−6.94 (m, 6H), 7.28−7.39 (m, 6H); ^{13}C NMR (100 MHz, $CDCl_3$) δ, 14.3, 22.9, 26.4, 29.6, 29.7, 30.6, 32.0, 41.7, 45.6, 48.2, 52.2, 56.2, 57.1, 76.1, 79.3, 82.4, 108.7, 109.8, 123.2, 123.3, 123.5, 123.8, 123.9, 124.9, 125.0, 134.7, 135.1, 135.4, 135.6, 144.8, 145.0, 145.1, 145.1, 145.3, 146.0, 147.0, 148.7, 149.1, 149.9; IR (KBr) 3297 (C≡C−H), 3068 (C═C−H), 2927 (C−H), 2105 (C≡C), 1580 (C═C) cm^{-1}; HRMS calcd for $C_{46}H_{42}O_3$, 642.3134; found, 642.3141.

Synthesis of Enantiopure 2OM. To a solution of 0.13 g (0.18 mmol) of **5OM** in 5 mL dry THF was added 1 mL of KOH(aq) and 5 mL of MeOH. The mixture was stirred at room temperature for 5 h. The reaction was quenched by 36.5% HCl(aq). The solvent was removed under reduced pressure, and the residue was dissolved in CH_2Cl_2 and washed with brine. The organic layer was dried over anhydrous $MgSO_4$, and the filtrate was concentrated under reduced pressure. To the residue was added 0.06 g (0.43 mmol) of potassium carbonate, 0.04 g (0.24 mmol) of potassium iodide, 0.1 mL (0.52 mmol) of 1-bromooctane, and 5 mL of dry DMF at room temperature for 10 h. The organic layer was added to 50 mL of water and extracted by CH_2Cl_2. Column chromatography with CH_2Cl_2/hexane (2:1) as eluent afforded the white solid of **2OM** with a yield of 76%: mp, 242−244 °C; $[\alpha]_D^{25}$ −9.8° (c = 1, CH_2Cl_2) and $[\alpha]_D^{25}$ +8.4° (c = 1, CH_2Cl_2) for enantiopure **2OM** from the first and the second HPLC elution of **5OM**, respectively.

Synthesis of 4OM. Under an atmosphere of argon, 1.0 mL of n-butyllithium in hexane (2.5 M, 2.5 mmol) was added dropwise to a solution of (trimethylsilyl)acetylene (0.30 mL, 2.2 mmol) in THF (15 mL) at −10 °C. The mixture was then kept at −10 °C for another 30 min before it was transferred to a solution of quinone **3OM** (1.0 g, 1.9 mmol) in THF (20 mL) at −10 °C. The mixture was stirred for 3 h at the same temperature before trimethylsilyl chloride (0.37 mL, 3.0 mmol), zinc powder (0.33 g, 5.1 mmol), and 2 mL of HOAc was added in this order. The mixture was warmed to room temperature and stirred for 24 h. The solvent was removed under reduced pressure, and the residue was dissolved in CH_2Cl_2 and washed with brine. The organic layer was dried over anhydrous $MgSO_4$, and the filtrate was concentrated under reduced pressure. To the residue was added 10 mL of dry THF

dx.doi.org/10.1021/jo2009017 |J. Org. Chem. 2011, 76, 5782–5792

and 3 mL of a solution of 10% KOH(aq) and 10 mL of MeOH. The mixture was stirred at room temperature for 5 h. The reaction was quenched by 36.5% HCl(aq). The solvent was removed under reduced pressure, and the residue was dissolved in CH_2Cl_2 and washed with brine. The organic layer was dried over anhydrous $MgSO_4$, and the filtrate was concentrated under reduced pressure. Column chromatography with CH_2Cl_2/hexane (2:1) as eluent afforded the white solid of racemic **4OM** with a yield of 33%: mp, >300 °C; ^{1}H NMR (400 MHz, $CDCl_3$) δ, 3.55 (s, 1H), 3.76 (s, 3H), 3.77 (s, 3H), 5.54 (s, 1H), 5.67 (s, 1H), 5.81 (s, 1H), 5.97 (s, 1H), 6.28 (s, 1H), 6.43−6.48 (m, 2H), 6.90−6.92 (m, 6H), 7.29−7.38 (m, 6H); ^{13}C NMR (100 MHz, $CDCl_3$) δ, 40.7, 45.6, 47.2, 52.1, 56.4, 57.1, 79.4, 81.8, 107.2, 109.1, 110.0, 123.4, 123.5, 123.9, 124.1, 125.0, 125.1, 125.1, 129.4, 129.7, 134.6, 135.5, 145.0, 145.0, 145.1, 145.1, 145.2, 145.4, 146.0, 146.5, 147.0, 148.5, 149.4; IR (KBr) 3438 (O−H), 3297 (C≡C−H), 3067 (C=C−H), 2937 (C−H), 2099 (C≡C), 1581 (C=C) cm^{-1}; HRMS calcd for $C_{38}H_{26}O_3$, 530.1882; found, 530.1864.

Synthesis of 5OM. To the solution of 0.27 g (1.4 mmol) of camphanic acid in 5.0 mL of THF was added 0.30 g (1.5 mmol) of dicyclohexylcarbodiimide, 0.02 g (0.16 mmol) of 4-(dimethylamino)pyridine, and 0.50 g (0.94 mmol) of racemic **4OM**, and the mixture was stirred for 12 h at room temperature. The solvent was removed under reduced pressure, and the residue was dissolved in CH_2Cl_2 and washed with brine. The organic layer was dried over anhydrous $MgSO_4$, and the filtrate was concentrated under reduced pressure. Column chromatography with CH_2Cl_2/hexane (3:1) as eluent afforded the white solid of diastereomeric **5OM** with a yield of 86%: mp, >300 °C; ^{1}H NMR (400 MHz, $CDCl_3$) δ, 1.31 (s, 6H), 1.43 (s, 6H), 1.48 (s, 6H), 2.01−1.93 (m, 2H), 2.23−2.13 (m, 2H), 2.61−2.51 (m, 2H), 2.96−2.82 (m, 2H), 3.64 (s, 2H), 3.70 (s, 3H), 3.71 (s, 3H), 3.79 (s, 6H), 5.26 (s, 1H), 5.30 (s, 1H), 5.81 (s, 2H), 5.86 (s, 2H), 6.31 (s, 2H), 6.50−6.42 (m, 4H), 6.97−6.6.90 (m, 12H), 7.25−7.20 (m, 6H), 7.41−7.35 (m, 6H); ^{13}C NMR (100 MHz, $CDCl_3$) δ, 9.8, 17.0, 17.1, 17.1, 29.0, 29.1, 31.4, 31.6, 42.0, 45.5, 48.8, 48.8, 52.0, 53.4, 54.5, 55.1, 55.9, 57.0, 78.6, 83.5, 91.2, 108.8, 108.9, 110.0, 112.2, 123.6, 123.7, 123.8, 123.9, 123.9, 124.1, 125.1, 125.3, 125.4, 125.4, 133.8, 134.4, 135.0, 135.0, 140.4, 143.9, 144.0, 144.0, 144.3, 144.4, 144.7, 144.7, 145.0, 145.0, 146.7, 147.5, 148.9, 149.2, 165.2, 165.2, 177.8, 177.9; IR (KBr) 3285 (C≡C−H), 2969 (C=C−H), 2249 (C≡C), 1795 (C=O), 1608 (C=C); HRMS calcd for $C_{48}H_{38}O_6$, 710.2668; found, 710.2668.

Separation of Diastereomers of 5OM. The mixture of diastereomeric **5OM** (0.05 g) in 3 mL of CH_2Cl_2 was separated by repeated HPLC (APS-2 Hypersil, 1:1 hexane/CH_2Cl_2 eluent, flow rate 10 mL/min). The retention time for the first and the second elution is 20−25 min and 23−28 min, respectively.

■ ASSOCIATED CONTENT

Supporting Information. 2D NMR spectra and complete VT NMR spectra for **1OM**-op, ^{1}H and ^{13}C NMR spectra of new compounds, AM1-derived rotational potentials and ethynyl bond angles for **1H**, **1OM**-*SS*$_2$, and **1OM**-*RS*$_2$, geared inter-rotor dihedral angle relationship for **1H**, and coordinates for the DFT- and AM1-calculated conformers and energies. This material is available free of charge via the Internet at http://pubs.acs.org.

■ AUTHOR INFORMATION

Corresponding Authors

*jsyang@ntu.edu.tw (J.-S.Y.); ichao@chem.sinica.edu.tw (I.C.).

■ ACKNOWLEDGMENT

We thank the National Science Council and Academia Sinica of Taiwan, ROC, for financial support. The computing time granted by the National Center for High-Performance Computing and the Computing Center of Academia Sinica is acknowledged.

■ REFERENCES

(1) (a) Kawada, Y.; Iwamura, H. *J. Org. Chem.* **1980**, *45*, 2547–2548. (b) Hounshell, W. D.; Johnson, C. A.; Guenzi, A.; Cozzi, F.; Mislow, K. *Proc. Natl. Acad. Sci. U.S.A.* **1980**, *77*, 6961–6964.

(2) (a) Iwamura, H.; Mislow, K. *Acc. Chem. Res.* **1988**, *21*, 175–182 and references therein. (b) Kawada, Y.; Kimura, Y.; Yamazaki, H.; Ishikawa, J.; Sakai, H.; Oguri, M.; Koga, G. *Chem. Lett.* **1994**, 1311–1314. (c) Setaka, W.; Nirengi, T.; Kabuto, C.; Kira, M. *J. Am. Chem. Soc.* **2008**, *130*, 15762–15763.

(3) Kawada, Y.; Sakai, H.; Oguri, M.; Koga, G. *Tetrahedron Lett.* **1994**, *35*, 139–142.

(4) (a) Bergman, J. J.; Chandler, W. D. *Can. J. Chem.* **1972**, *50*, 353–363. (b) Clayden, J.; Pink, J. H. *Angew. Chem., Int. Ed.* **1998**, *37*, 1937–1939. (c) Bragg, R. A.; Clayden, J. *Org. Lett.* **2000**, *2*, 3351–3354. (d) Hiraoka, S.; Okuno, E.; Tanaka, T.; Shiro, M.; Shionoya, M. *J. Am. Chem. Soc.* **2008**, *130*, 9089–9098. (e) Nikitin, K.; Müller-Bunz, H.; Ortin, Y.; Risse, W.; McGlinchey, M. J. *Eur. J. Org. Chem.* **2008**, 3079–3084. (f) Ściebura, J.; Skowronek, P.; Gawronski, J. *Angew. Chem., Int. Ed.* **2009**, *48*, 7069–7072.

(5) (a) Kottas, G. S.; Clarke, L. I.; Horinek, D.; Michl, J. *Chem. Rev.* **2005**, *105*, 1281–1376. (b) Kay, E. R.; Leigh, D. A.; Zerbetto, F. *Angew. Chem., Int. Ed.* **2007**, *46*, 72–191.

(6) (a) Stevens, A. M.; Richards, C. J. *Tetrahedron Lett.* **1997**, *38*, 7805–7808. (b) Carella, A.; Launay, J.-P.; Poteau, R.; Rapenne, G. *Chem.—Eur. J.* **2008**, *14*, 8147–8156. (c) Ogi, S.; Ikeda, T.; Wakabayashi, R.; Shinkai, S.; Takeuchi, M. *Chem.—Eur. J.* **2010**, *16*, 8285–8290.

(7) (a) Hart, H.; Shamouilian, S.; Takehira, Y. *J. Org. Chem.* **1981**, *46*, 4427–4432. (b) Hart, H.; Bashir-Hashemi, A.; Luo, J.; Meador, M. A. *Tetrahedron* **1986**, 1641–1654.

(8) Yang, J.-S.; Yan, J.-L. *Chem. Commun.* **2008**, 1501–1512.

(9) (a) Yang, J.-S.; Ko, C.-W. *J. Org. Chem.* **2006**, *71*, 844–847. (b) Yang, J.-S.; Yan, J.-Y.; Jin, Y.-X.; Sun, W.-T.; Yang, M.-C. *Org. Lett.* **2009**, *11*, 1429–1432. (c) Kundu, S. K.; Tan, W. S.; Yan, J.-L.; Yang, J.-S. *J. Org. Chem.* **2010**, *75*, 4640–4643.

(10) Yang, J.-S.; Yan, J.-L.; Hwang, C.-Y.; Chiou, S.-Y.; Liau, K.-L.; Tsai, H.-H. G.; Lee, G.-H.; Peng, S.-M. *J. Am. Chem. Soc.* **2006**, *128*, 14109–14119.

(11) Yang, J.-S.; Swager, T. M. *J. Am. Chem. Soc.* **1998**, *120*, 11864–11873.

(12) Zhu, X.-Z.; Chen, C.-F. *J. Org. Chem.* **2005**, *70*, 917–924.

(13) Toyota, S.; Shimizu, T.; Iwanaga, T.; Wakamatsu, K. *Chem. Lett.* **2011**, *40*, 312–314.

(14) Kelly, T. R.; Bowyer, M. C.; Bhaskar, K. V.; Bebbington, D.; Garcia, A.; Lang, F.; Kim, M. H.; Jette, M. P. *J. Am. Chem. Soc.* **1994**, *116*, 3657–3658.

(15) Elangovan, A.; Wang, Y.-H.; Ho, T.-I. *Org. Lett.* **2003**, *5*, 1841–1844.

(16) Siemsen, P.; Livingston, R. C.; Diederich, F. *Angew. Chem., Int. Ed.* **2000**, *39*, 2632–2657.

(17) Kendhale, A. M.; Poniman, L.; Dong, Z.; Laxmi-Reddy, K.; Kauffmann, B.; Ferrand, Y.; Huc, I. *J. Org. Chem.* **2011**, *76*, 195–200.

(18) Eliel, E. L.; Wilen, S. H.; Doyle, M. P. *Basic Organic Stereochemistry*; Wiley-Interscience: New York, 2001.

(19) Becke, A. D. *J. Chem. Phys.* **1993**, *98*, 5648–5652. All calculations were carried out using G03 software.

(20) For a previous example of ungeared rocking motions, see: Hirose, K.; Ishibashi, K.; Shiba, Y.; Doi, Y.; Tobe, Y. *Chem.—Eur. J.* **2008**, *14*, 5803–5811.

(21) Szafert, S.; Gladysz, J. A. *Chem. Rev.* **2003**, *103*, 4175–4205.

(22) The ring current of anisole has been suggested to be similar or slightly larger than that of benzene, see: Stamm, H.; Jäckel, H. *J. Am. Chem. Soc.* **1989**, *111*, 6544–6550.

(23) (a) Frisch, M. J.; Trucks, G. W.; Schlegel, H. B.; Scuseria, G. E.; Robb, M. A.; Cheeseman, J. R.; Montgomery, J. A., Jr.; Vreven, T.; Kudin, K. N.; Burant, J. C.; Millam, J. M.; Iyengar, S. S.; Tomasi, J. J.; Barone, V.; Mennucci, B.; Cossi, M.; Scalmani, G.; Rega, N.; Petersson, G. A.; Nakatsuji, H.; Hada, M.; Ehara, M.; Toyota, K.; Fukuda, R.;

Hasegawa, J.; Ishida, M.; Nakajima, T.; Honda, Y.; Kitao, O.; Nakai, H.; Klene, M.; Li, X.; Knox, J. E.; Hratchian, H. P.; Cross, J. B.; Adamo, C.; Jaramillo, J.; Gomperts, R.; Stratmann, R. E.; Yazyev, O.; Austin, A. J.; Cammi, R.; Pomelli, C.; Ochterski, J. W.; Ayala, P. Y.; Morokuma, K.; Voth, A.; Salvador, P.; Dannenberg, J. J.; Zakrzewski, V. G.; Dapprich, S.; Daniels, A. D.; Strain, M. C.; Farkas, O.; Malick, D. K.; Rabuck, A. D.; Raghavachari, K.; Foresman, J. B.; Ortiz, J. V.; Cui, Q.; Baboul, A. G.; Clifford, S.; Cioslowski, J.; Stefanov, B. B.; Liu, G.; Liashenko, A.; Piskorz, P.; Komaromi, I.; Martin, R. L.; Fox, D. J.; Keith, T.; Al-Laham, M. A.; Peng, C. Y.; Nanayakkara, A.; Challacombe, M.; Gill, P. M. W.; Johnson, B.; Chen, W.; Wong, M. W.; Gonzalez, C.; Pople, J. A. *Gaussian 03*, revisions D.02 and E.01; Gaussian, Inc.: Wallingford, CT, 2004. (b) Frisch, M. J.; Trucks, G. W.; Schlegel, H. B.; Scuseria, G. E.; Robb, M. A.; Cheeseman, J. R.; Scalmani, G.; Barone, V.; Mennucci, B.; Petersson, G. A.; Nakatsuji, H.; Caricato, M.; Li, X.; Hratchian, H. P.; Izmaylov, A. F.; Bloino, J.; Zheng, G.; Sonnenberg, J. L.; Hada, M.; Ehara, M.; Toyota, K.; Fukuda, R.; Hasegawa, J.; Ishida, M.; Nakajima, T.; Honda, Y.; Kitao, O.; Nakai, H.; Vreven, T.; Montgomery, J. A., Jr.; Peralta, J. E.; Ogliaro, F.; Bearpark, M.; Heyd, J. J.; Brothers, E.; Kudin, K. N.; Staroverov, V. N.; Kobayashi, R.; Normand, J.; Raghavachari, K.; Rendell, A.; Burant, J. C.; Iyengar, S. S.; Tomasi, J.; Cossi, M.; Rega, N.; Millam, N. J.; Klene, M.; Knox, J. E.; Cross, J. B.; Bakken, V.; Adamo, C.; Jaramillo, J.; Gomperts, R.; Stratmann, R. E.; Yazyev, O.; Austin, A. J.; Cammi, R.; Pomelli, C.; Ochterski, J. W.; Martin, R. L.; Morokuma, K.; Zakrzewski, V. G.; Voth, G. A.; Salvador, P.; Dannenberg, J. J.; Dapprich, S.; Daniels, A. D.; Farkas, Ö.; Foresman, J. B.; Ortiz, J. V.; Cioslowski, J.; Fox, D. J. *Gaussian 09*, revision A.2; Gaussian, Inc.: Wallingford, CT, 2009.